Technical Innovations & Patient Support in Radiation Oncology 29 (2024) 100236

Contents lists available at ScienceDirect

Technical Innovations & Patient Support in Radiation Oncology

journal homepage: www.sciencedirect.com/journal/technical-innovations-and-patient-support-in-radiation-oncology

Research article

Are offline ART decisions for NSCLC impacted by the type of dose calculation algorithm?

Dylan Callens [a,b,*], Karel Aerts [a], Patrick Berkovic [a,b], Liesbeth Vandewinckele [a,b], Maarten Lambrecht [a,b], Wouter Crijns [a,b]

[a] Laboratory of Experimental Radiotherapy, KU Leuven, Leuven, Belgium
[b] Department of Radiation Oncology, UZ Leuven, Leuven, Belgium

ARTICLE INFO

Keywords:
NSCLC
Dose calculation
Adaptive radiotherapy

ABSTRACT

Introduction: Decisions for plan-adaptations may be impacted by a transitioning from one dose-calculation algorithm to another. This study examines the impact on dosimetric-triggered offline adaptation in LA-NSCLC in the context of a transition from superposition/convolution dose calculation algorithm (Type-B) to linear Boltzmann equation solver dose calculation algorithms (Type-C).

Materials & Methods: Two dosimetric-triggered offline adaptive treatment workflows are compared in a retrospective planning study on 30 LA-NSCLC patients. One workflow uses a Type-B dose calculation algorithm and the other uses Type-C. Treatment plans were re-calculated on the anatomy of a mid-treatment synthetic-CT utilizing the same algorithm utilized for pre-treatment planning. Assessment for plan-adaptation was evaluated through a decision model based on target coverage and OAR constraint violation. The impact of algorithm during treatment planning was controlled for by recalculating the Type-B plan with Type-C.

Results: In the Type-B approach, 13 patients required adaptation due to OAR-constraint violations, while 15 patients required adaptation in the Type-C approach. For 8 out of 30 cases, the decision to adapt was opposite in both approaches. None of the patients in our dataset encountered CTV-target underdosage that necessitated plan-adaptation. Upon recalculating the Type-B approach with the Type-C algorithm, it was shown that 10 of the original Type-B plans revealed clinically relevant dose reductions ($\geq$3%) on the CTV in their original plans. This re-calculation identified 21 plans in total that required ART.

Discussion: In our study, nearly one-third of the cases would have a different decision for plan-adaption when utilizing Type-C instead of Type-B. There was no substantial increase in the total number of plan-adaptations for LA-NSCLC. However, Type-C is more sensitive to altered anatomy during treatment compared to Type-B. Recalculating Type-B plans with the Type-C algorithm revealed an increase from 13 to 21 cases triggering ART.

Introduction

In modern radiotherapy, various dose calculation algorithms are considered standard for treatment planning. There are **Type-B** algorithms, known as the superposition/convolution algorithms, including the Anisotropic Analytical Algorithm (AAA, Varian a Siemens Healthineers Company, Eclipse™ treatment planning system), which is often used [1]. Additionally, there are **Type-C** algorithms, known as linear Boltzmann transport equation (LBTE) solvers, which include the frequently used Acuros XB algorithm (AXB, Varian a Siemens Healthineers Company, Eclipse™ treatment planning system) [2]. The dose calculation algorithms, with their specific characteristics, are becoming increasingly important due to the growing implementation of online and offline adaptive radiotherapy (ART) strategies. In online adaptive treatment units, systems can operate independently from the department's regular treatment planning systems and may employ different algorithms [3]]. For offline adaptive strategies, decisions to adapt the original treatment plan are typically triggered by geometric changes [4,5], dosimetric changes [6,7], or a combination of both [8]. In cases where the decision to adapt the treatment is based on dosimetric changes by utilizing the daily ConeBeam CT imaging (CBCT), the choice of dose calculation algorithm may play a critical role in this decision-making process. This can be particularly important when adapting plans for lung cancer, an indication with a substantial clinical interest in

* Corresponding author.
E-mail address: dylan.callens@uzleuven.be (D. Callens).

https://doi.org/10.1016/j.tipsro.2024.100236
Received 18 August 2023; Received in revised form 3 January 2024; Accepted 9 January 2024
Available online 12 January 2024

adapting more frequently for potential clinical benefits [4,9–11]. Lung cancer treatments involve various density changes throughout the course of treatment and are complicated by respiratory motion [4,12–14].

In the context of Type-B planning workflows, it has been observed that in lung cancer pre-treatment planning, there is generally acceptable accuracy but with potential overestimation of dose in air and limited accuracy errors near lung/soft-tissue interfaces [1,15–17]. In Type-C planning workflows, it is known that these algorithms are a compatible alternative to Monte Carlo methods in terms of reliable dose calculations in the vicinity of tissue heterogeneities [18–20]. However, these observed dose differences are minimal and not always clinically or statistically significant in pre-treatment planning because convolution algorithms (Type-B) are highly effective and accurate in most cases [18]. Though, LBTE-solver algorithms (Type-C) could perform slightly better in dose calculation in tissues with significant density variations [18].

The transition from using a Type-B algorithm to a Type-C algorithm in pre-treatment planning is well-documented [21–24]. In addition, the Global Quality Assurance of Radiation Therapy Clinical Trials Harmonisation Group has recommended the use of advanced dose-to-medium calculations, such as offered in Type-C in clinical trials and practice, whenever feasible [25]. What has not been thoroughly investigated, in the era of increased plan-adaptations, is the extent to which the dose calculation algorithm impacts the decision to adapt the plan. This is particularly relevant in lung cancer, where there is a strong interest in conducting more adaptations, and where both algorithms are still commonly used despite revealed differences in dose calculations. In lung radiotherapy treatment planning, dose gradients are planned close to tissue borders, and altered anatomy such as atelectasis or pleural effusion are common. Our study aims to assess the impact of the dose calculation algorithm on a dosimetric-triggered decision for plan-adaptation in patients with LA-NSCLC. The primary question is to what extent Type-C algorithms will reveal more cases that require adaptation compared to Type-B algorithms.

Materials and methods

Patient characteristics

This retrospective study included 30 patients diagnosed with LA-NSCLC. The patients received either concurrent or sequential chemo-radiotherapy. Specific patient and treatment characteristics are shown in Table 1. All treatments were administered between February 2021 and August 2022. The cases were randomly selected from a larger database of all LA-NSCLC patients treated during that time period at the Radiation Oncology unit of the University Hospital of Leuven. The manuscript is written based on the RAdiotherapy Treatment plannINg study Guidelines (RATING)[1] [26].

Treatment preparation

All cases have followed the standard clinical flow. A 4D planning-CT was acquired while patients maintained a reproducible position with the arms upright. Two patients had a lesion in the lung apex, which required an alternative posture with the arms placed next to the body, along with a five-point thermoplastic mask. The planning-CT was conducted utilizing either Somatom Definition Edge or Somatom Drive *(Siemens Healthineers, Erlangen, Germany)*.

Target volumes involving the primary tumor and lymph nodes were delineated on the mean intensity projection (MeanIP) of the 4D planning-CT based upon international guidelines [27,28]). To ensure appropriate treatment coverage, a planning target volume (PTV) of seven millimeter was created around the clinical target volume (CTV).

Table 1
Patient, tumor and treatment characteristics.

NSCLC Cases n = 30		
Patient and treatment characteristics	Gender	
	• M	22
	• F	8
	Age	
	• Mean ± SD	67 ± 10
	• Range	42–84
	Location of primary GTV	
	• Left	12
	• Right	18
	Prescribed fractionation scheme for PTV_{total}	
	• 66 Gy/2Gy	11
	• 60 Gy/2Gy	9
	• 63.25 Gy/2.75 Gy	2
	• 60.5 Gy/2.75 Gy	3
	• 55 Gy/2.75 Gy	5
Tumor characteristics	Tumor type	
	• Adenocarcinoma	15
	• Squamous	15
	Stage	
	• Stage III/Stage IV	25–5
	Volume of primary GTV (cm^3) (n = 30)	
	• Mean ± SD	65 ± 94
	• Range	2–462
	Volume of nodular GTV (cm^3) (n = 26)	
	• Mean ± SD	11 ± 15
	• Range	1–76

Organs at risk (OAR) were also delineated on the MeanIP. Several delineations of OAR included an isotropic planning risk volume (PRV). A five millimeter PRV around brachial plexi, mediastinal envelope and esophagus was created, for the spinal canal the PRV was limited to three millimeter. Two radiation oncologists delineated all structures.

Treatment planning

In Fig. 1 an overview of the treatment planning workflows are depicted. For the treatment planning, two separate workflows were introduced to create the two distinct planning approaches for comparison: the **Type-B planning workflow** and the **Type-C planning workflow**. Both workflows start using the same pre-existing in-house developed IMRT class solution with nine 6MV-FFF beams, which was designed for Halcyon™ *(Varian, a Siemens Healthineers Company, Palo Alto, CA)*. The distinct planning workflows are optimized independently and blinded of each other. This optimization process utilizes Varian's knowledge-based planning tool, RapidPlan™. The tool was used for predicting the expected dose-volume histograms (DVHs) before manually fine-tuning the optimization.

The optimization process, using the photon-optimizer (PO) v16.1.0 algorithm, was followed by the dose calculation. The dose calculation in the **Type-B** workflow utilizes AAA version 16.1.0 algorithm, whereas in the **Type-C** workflow, the AcurosXB algorithm version 16.1.0 is used.

In both treatment planning workflows, the calculation grid size (CGS) was set on 2.5 mm as this is common for IMRT [29], resulting in a balanced trade-off between feasible calculation time and potential dose inaccuracies. All plans were normalized on the target mean.

The main focus of the research is the interference between the altered intra-thoracic anatomy and the sensitivity of the utilized algorithm. However, differences may also be induced during treatment planning due to the selected algorithm. To asses the impact of such planning bias in the current work, the initial Type-B plan is recalculated without re-optimization or normalization using the Type-C algorithm. This will be referred to as the Control test.

[1] *The accompanying score sheet can be found in appendix.*

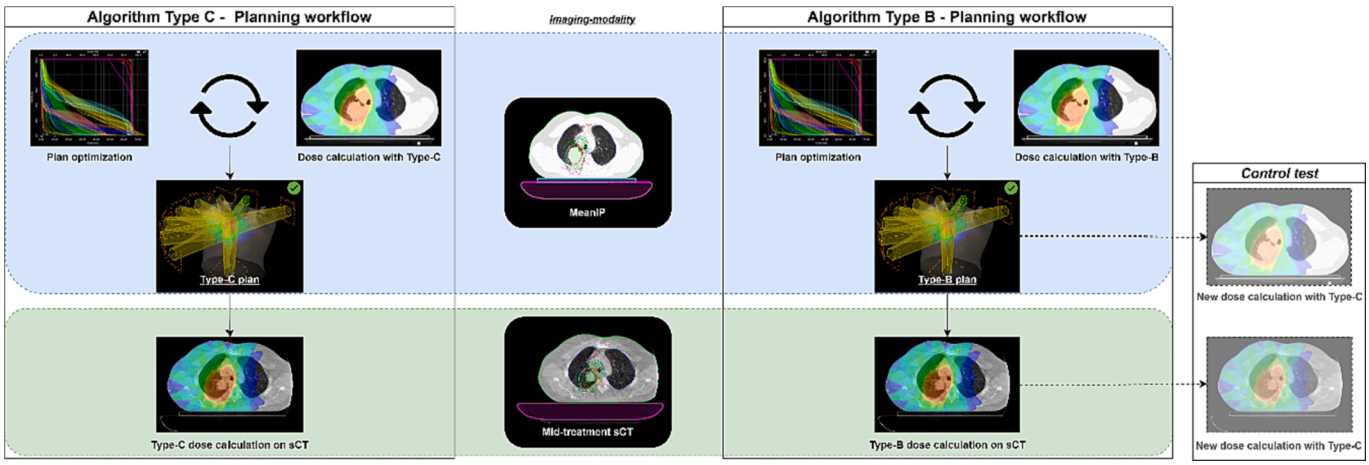

Fig. 1. Overview of the two investigated treatment planning workflows. On the left side of the figure, the Type-C planning workflow can be observed. A plan optimization is initiated, followed by a dose calculation. This entails an iterative procedure. Upon acceptance based on DVH parameters and multidisciplinary approval, the Type-C plan is obtained. This plan is copied on the mid-treatment sCT, where only a dose calculation is performed on the anatomy-of-the-day. The Type-B workflow, situated in the right of the figure, unfolds entirely analogously. To asses the effect of a potential planning bias between workflows the Type-B plans are re-calculated with the Type-C algorithm for both the pre-treatment planning and mid-treatment assessment (Control test, righ panel).

Treatment plan evaluation

For both planning workflows, a plan was deemed clinically acceptable based upon ICRU and QUANTEC recommendations *(see* Table 2*)*. Target coverage was prioritized. Only the maximum dose to the mediastinum or esophagus could be exceeded if it was necessary to achieve adequate target coverage. The decision in this regard was made through a multidisciplinary approach. All remaining constraints and target coverages were required to be met. Plans were clinically validated in retrospect.

Dosimetric-triggered ART assessment

For this study, the research question will be evaluated using mid-treatment imaging, as this particular time point is considered beneficial for adapting the treatment plan in lung cancer [30]. Instead of the time-consuming and repeated 4DCT involving additional imaging radiation, the mid-treatment CBCT is used. To address the inferior image quality of the CBCT, a synthetic-CT was generated through MIM *(MIM Software Inc, Cleveland, OH)* using deformable image registration through an intensity based, free-form cubic spline interpolation algorithm. The planning CT was deformed to match the geometry of the CBCT. Due to the limited field of view of the acquired CBCT for radiation protection reasons, only the region covered by the CBCT was deformed, and the rest of the planning CT was aligned to this deformation. This sCT-approach has been proven valid [11,31]. For our study, the GTV's and OAR of the planning-CT were deformed according the deformation vectors and manually adjusted. An isotropic five millimeter CTV and seven millimeter PTV margin were added.

For both planning workflows (Type-B and Type-C), the plans were duplicated and re-calculated without re-optimization on the mid-treatment sCT. Similar to the control test in pre-treatment planning, the Type-B plan was additionally re-calculated onto the sCT with the Type-C algorithm.

LungART decision-guide

A plan-adaptation decision-guide model has been created in this study based on our current original planning *wishlist* for OAR constraints *(cf.* Table 2*)*. This planning wishlist also serves as the foundation for the IGRT-traffic light protocol (TLP) used by the RTT for daily CBCT-imaging registration. In this TLP, the PTV is considered less important compared to the CTV, which is also reflected in the wishlist of the current ART-model. For evaluation of this constraint, the recommendation for CTV coverage by Hoffmann et al (2017) was retained [7]. Furthermore, the TLP guides the RTT towards a mediastinal envelop image-registration with verification of the tumor, spinal cord and lungs. These steps are also reflected in the decision-guide model. The P1-and P2-constraints in the decision-guide are considered hard constraints within the original planning. The P3-constraints are soft constraints.

A recommendation with high priority (P1, *high recommendation*) is defined as the immediate need for replanning due to inadequate coverage of the clinical target volume (CTV). If the dose limits for the spinal cord, mean lung, and heart are exceeded, a recommendation with normal priority is given (P2, *normal recommendation*). In instances of high workload within the department, adaptive treatment planning can then be delayed for a maximum of two treatment fractions. If the esophagus and mediastinal envelope receive an intolerable dose that was not anticipated during the planningCT, the patient may continue treatment without plan-adaptation, but the case should be closely monitored (P3, *low recommendation*). If there is capacity within the dosimetry department for plan-adaptation, it is recommended to adapt the plan.

The designed model can be found in Fig. 2.

Assessment metrics

The two planning workflows will be compared through the decision model. This model identifies the number of cases for adaptation based on CTV underdosage and overdosage on OAR (Fig. 2). In addition to the LungART decision guide, we will assess all clinical constraints used in pre-treatment planning as detailed in Table 2. Dose differences on these clinical constraints between mid-treatment and original treatment planning will be evaluated on a ± 3 % threshold-value which is considered as clinical relevant. This threshold has been previously used as metric in algorithm comparison studies [32,33] Notably, this threshold is more stringent than the clinically relevant 5 % dose difference acknowledged in Report 85 of the American Association of Physicists in Medicine (AAPM) [34].

The supplementary material provides additional dosimetric analyses and a case-by-case analysis.

Results

Dosimetric-triggered ART assessment

For this retrospective study on 30 patients LA-NSCLC, the need for adaptation was evaluated for each planning workflow (**Type-B** and

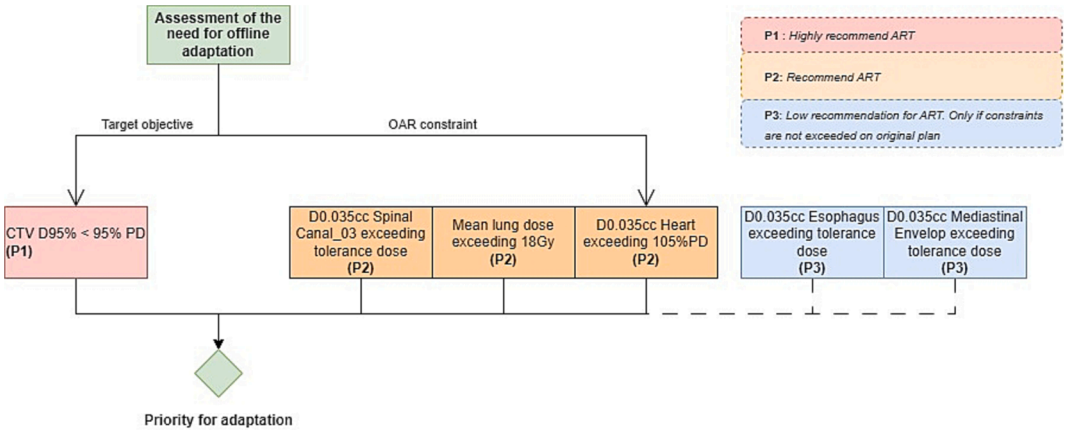

Fig. 2. Criteria for Adaptation protocol.

Table 2
Target objectives and OAR constraints for NSCLC.

Prescribed dose (PD)		60/66 Gy-2 Gy	63.25 Gy-2.75 Gy	60.5 Gy-2.75 Gy	55 Gy-2.75 Gy
Priority	**Structure**	**Objective**			
Most Important	**PTV**	D95.0 % ≥ 95.0 % PD D0.035 cm^3 ≤ 115.0 % PD			
Very Important	**PTV**	D99.0 % ≥ 90.0 % PD			
	SpinalCanal_03	D0.035 cm^3 < 50.00 Gy	D0.035 cm^3 < 48.50 Gy	D0.035 cm^3 < 48.00 Gy	D0.035 cm^3 < 46.00 Gy
Important	**Esophagus_05**	D0.035 cm^3 < 100.0 %	D0.035 cm^3 < 60.40 Gy	D0.035 cm^3 < 58.00 Gy	D0.035 cm^3 < 52.50 Gy
	MediastinalEnvelope_05	D0.035 cm^3 < 105.0 %	D0.035 cm^3 < 65.00 Gy	D0.035 cm^3 < 64.00 Gy	D0.035 cm^3 < 62.00 Gy
	Brachial_Plexi_05	D0.035 cm^3 < 105.0 %	D0.035 cm^3 < 62.50 Gy	D0.035 cm^3 < 61.50 Gy	D0.035 cm^3 < 59.50 Gy
	Heart	D_Mean < 20.00 Gy D0.035 cm^3 < 105.0 % PD			
	Lungs	D_Mean < 18.00 Gy			
Least Important	**Contralateral Lung**	V5.00 Gy < 50.0 % PD			
Additional reported dose objectives	***CTV***	*D95.0 % ≥ 95.0 % PD* *D99.0 % ≥ 90.0 % PD* *D_Mean = ± 1 Gy*			

Type-C) through our LungART decision-guide model. As demonstrated in Table 3, when utilizing a Type-B algorithm in the **Type-B ART-decision workflow**, the decision-guide for ART reveals 13 out of 30 cases for adaptation. In a **Type-C workflow** 15 out of 30 cases would have been adapted. Within these cases, there were 10 plans where the same decision would be made to modify the plan. In 12 of the 30 plans, the same decision would be made to continue the original treatment plan. In 8 of the 30 plans, an opposite decision would have been made within the two distinct planning workflows.

Table 3
Assessment of the need for offline adaptation. Within the planning workflows, the number of plans that should be adapted for each recommendation grade is displayed based on the mentioned specific criteria. The common plans include only Type-B and Type-C plans, without incorporating the Control test. *Compared to Type-B original plan.

Planning workflow	**Number of plan-adaptations**			
	Type-B	**Type-C**	***Common***	***Control test***
P1: CTV coverage	0	0	/	*10*
P2: Spinal Canal exceeding tolerance dose	2	3	2	*1*
P2: Mean lung dose exceeding tolerance dose	0	0	/	*0*
P2: Heart exceeding tolerance dose	5	5	3	*4*
P3: Esophagus exceeding tolerance dose *(not on original plan)*	7	5	2	*8**
P3: Mediastinal envelop exceeding tolerance dose *(not on original plan)*	7	8	4	*11**
Total plans to adapt *(in some cases dose violations occur on several constraints)*	**13**	**15**	**10**	***21***
Unique additional adaptations	**3**	**5**		

The P2-recommendation for ART due to a violation of a maximal voxel dose on the spinal canal occurred in 2 cases for the **Type-B flow**. The violation was found in 3 cases for the **Type-C flow**. Two cases were common amongst both planning approaches. The P2-recommendation due to the mean lung dose constraint violation did not occur. In both planning flows, 5 P2-recommendations were due to heart dose violations.

The dose constraint on the mediastinal envelope and esophagus is frequently violated (P3), both in the **Type-B and Type-C flow**. It can be observed that the P3-recommendation, resulting from a dose violation on the esophagus and mediastinal envelop *(in contrary with the Type-B original plan)*, occurs more frequently in the Control test.

In the Control test, 10 cases had a P1-recommendation for adaptation compared to none in the distinct Type-B and Type-C planning workflows. Adding up all recommendations for adaptation in these series, this resulted in the identification of an increase from 13 to 21 plans that would require adaptation when compared to the original Type-B plan.

Mid-treatment vs. pre-treatment dose constraint values

In total, there were 514 constraints that could be met considering all cases, as indicated in Table 4. More constraints were met in the **Type-B flow** compared to the **Type-C flow** (496 vs. 470). In line with these observations, it is shown that more plans were without constraint violation in the **Type-B flow** (18 vs. 6 in the **Type-C flow**). Especially note that for the Type-B plans in pre-treatment planning, 18 plans can be

Table 4
Met constraints and total number of plans without constraint violations across planning workflows. The evaluation using the Control test involved comparing the results with the originally created Type-B plans. *Compared to the original Type-B flow.

Planning workflow	**Original plan**			**Calculated on sCT**		
	Type-B flow	**Type-C flow**	**Control test**	**Type-B flow**	**Type-C flow**	**Control test**
Constraints met (n = 514 total constraints) ***Decrease of met constraints****	496 [96 %]	470 [91 %]	378 [74 %] *−118**	420 [81 %] −74	392 [76 %] −75	359 [70 %] −40
Total number of plans without constraint violations (n = 30)	18	6	1	3	3	1

depicted without constraint violations. The Control test, however, revealed that only 1 out of 30 plans in the Type-B flow had no constraint violations. Furthermore, we observe that 378 or 74 % of the constraints were met.

Similar results are observed in the mid-treatment-calculations. Within the **Type-B flow** more constraints were met than the **Type-C flow** (420 vs. 392). When evaluating the number of constraints that were met during mid-treatment assessment, in addition to the initially met constraints, we observe a difference of one additional constraint violation between **Type-B** and **Type-C** (respectively 74 and 75 additional constraint violations compared to the original plans). The Control test led to 70 % met constraints. Forty additional constraints, on top of 118 violated in the planning control test.

The mid-treatment constraint values compared to the pre-treatment dose constraint values for each planning workflow (Type-B, Type-C and Control test) are presented in boxplot figures (Fig. 3 and Fig. 5).

In Fig. 3, it is illustrated that no clinically relevant underdosage of 3 % is observed on CTVp D95% in both planning workflows. For the CTVn D95%, there is one case in the Type-B flow with a clinically relevant underdose on CTVn D95%. The control test reveals 9 cases with clinically relevant underdosage on CTVp D95% and 21 cases with a clinically relevant underdosage on CTVn D95%. Concerning PTV-volumes, particularly those encompassing lymph nodes, larger underdosages of more than 3 % are frequently noted in both planning workflows. These discrepancies are attributed to inferior coverage on PTV volumes resulting from altered anatomy. In regard to this, a specific case stands out where the PTVn D99% in both Type-B and Type-C mid-treatment calculations has an outlier of −100 %, primarily due to a large noticeable mediastinal shift.

The underdosages on CTVp and CTVn in the Type-B planning workflows are illustrated through a case with dose line profiles in Fig. 4. Herein it can be observed that the Type-B algorithm results in an overestimation of the dose in heterogeneous tissue in for example the bronchial tree and trachea, unlike Type-C, where a more accurate dose calculation is presented without overestimation of the dose in lung tissue.

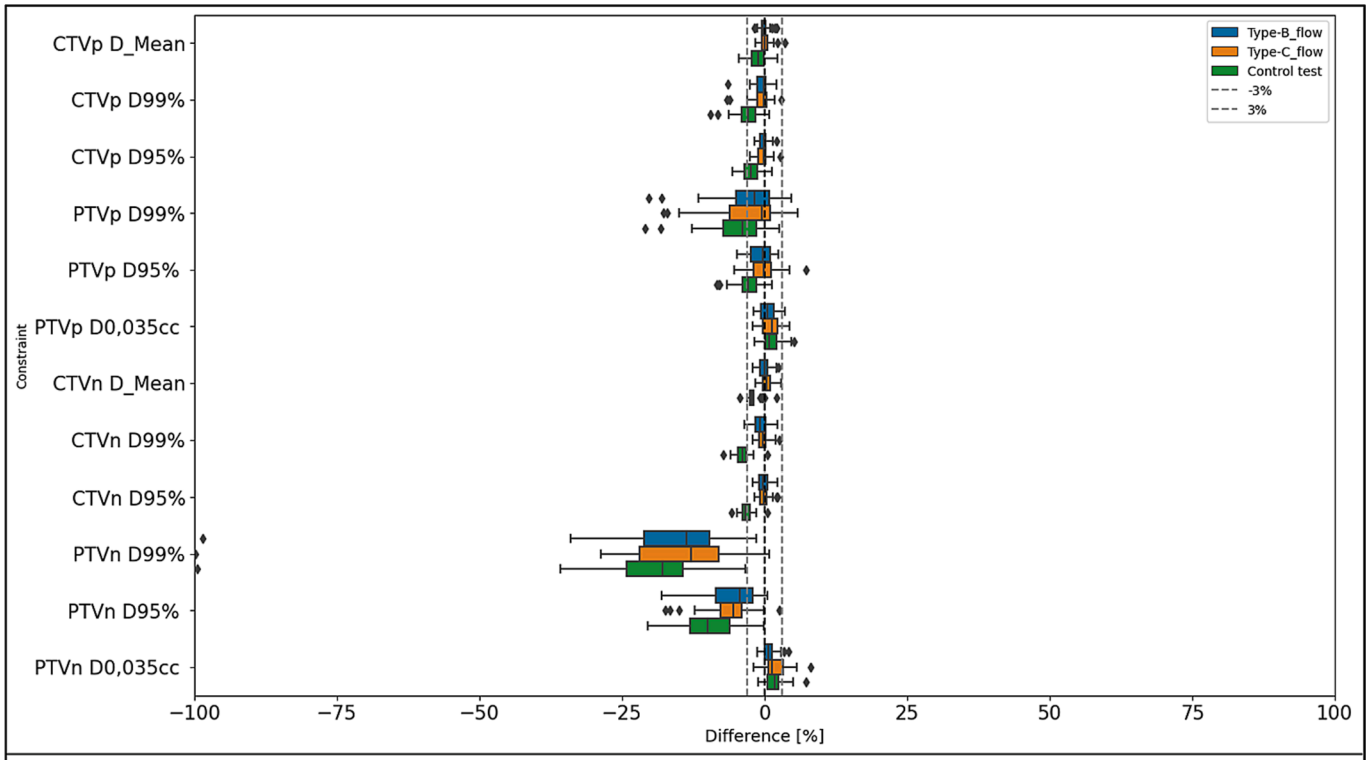

Amount of cases (n=30)	CTVp_05						CTVn_05						PTVp_07						PTVn_07					
	D_Mean		D99%		D95%		D_Mean		D99%		D95%		D99%		D95%		D0,035cc		D99%		D95%		D0,035cc	
	-3%Δ	+3%Δ	-3%Δ	+3%Δ	-3%Δ	+3%Δ	-3%Δ	+3%Δ	-3%Δ	+3%Δ	-3%Δ	+3%Δ	-3%Δ	+3%Δ	-3%Δ	+3%Δ	-3%Δ	+3%Δ	-3%Δ	+3%Δ	-3%Δ	+3%Δ	-3%Δ	+3%Δ
Type-B flow	0	0	1	0	0	0	0	0	1	0	0	0	12	2	4	0	0	1	25	0	17	0	0	2
Type-C flow	0	1	3	0	0	0	0	0	0	0	0	0	12	4	4	3	0	6	24	0	21	0	0	7
Control test	*4*	*0*	*14*	*0*	*9*	*0*	*4*	*0*	*21*	*0*	*18*	*0*	*18*	*0*	*14*	*0*	*0*	*7*	*26*	*0*	*25*	*0*	*0*	*5*

Fig. 3. Boxplots of the target doses in the mid-treatment calculated plans compared to the original treatment plans. The figure is complemented by the number of cases in both planning workflows and the Control test, having a ± 3 % dose difference per constraint.

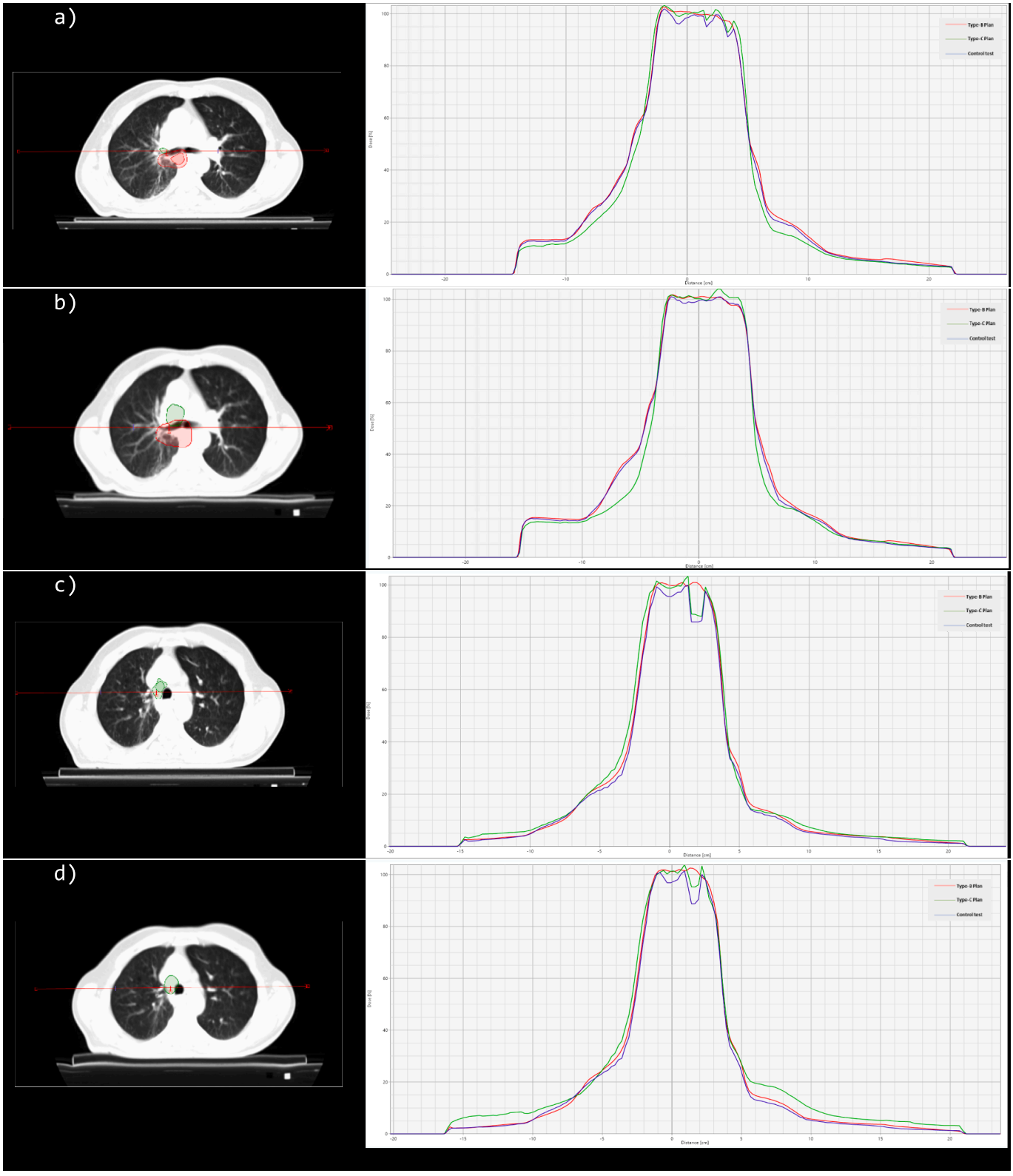

Fig. 4. Dose line profile at the location of the isocenter and cranially at the nodular CTV lateral to the trachea. The red line represents the dose profile of the Type-B plan, the green line corresponds to the Type-C plan, and the blue line represents the Control test. a) MeanIP at the isocenter. It is observed that a Type-C calculation on the Type-B plan clearly indicates a more limited dose coverage on the target compared to the Type-C plan. Note that the Type-B plan shows a more linear dose profile despite the passage through air, as revealed in Type-C and the Control Test. The control test suggests that Type-B overestimates the dose in heterogeneous tissue.b) sCT at the isocenter. Similar dose profiles with minimal differences.c) MeanIP at the nodular CTV. Take note of the air in the trachea, which Type-B barely considers. In the control test and Type-C plan, a distinct bend in the dose is observed. d) sCT at the nodular CTV. Similar dose profiles as the planningCT. However, observe the dose peak just after tracheal air, as demonstrated in Type-C flow and the control test. (For interpretation of the references to colour in this figure legend, the reader is referred to the web version of this article.)

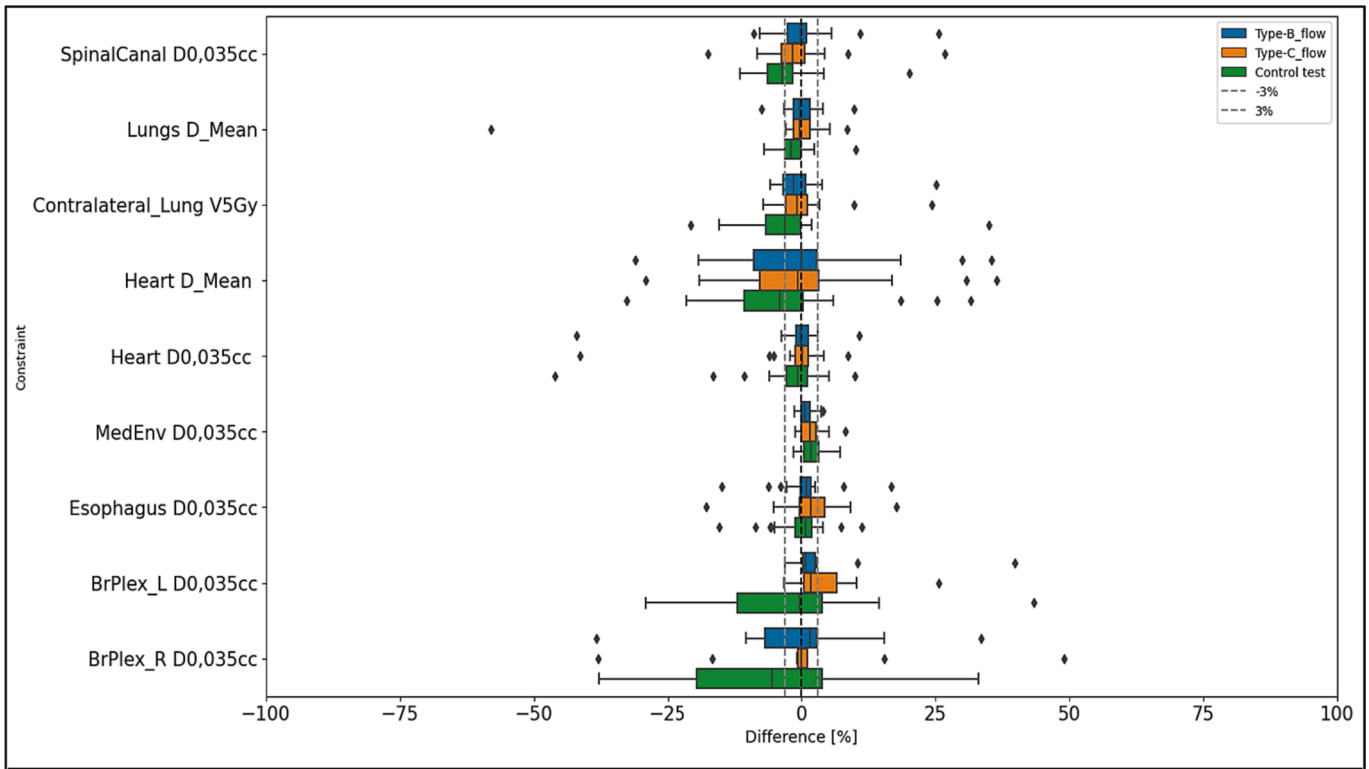

Amount of cases (n=30)	Spinal Canal D0,035cc		Lungs-GTV D_Mean		Contralat_Lung V5Gy		Heart D_Mean		Heart D0,035cc		Mediast Envelop D0,035cc		Esophagus D0,035cc		Brachial Plex L D0,035cc		Brachial Plex R D0,035cc	
	-3% Δ	3% Δ	-3% Δ	3% Δ	-3% Δ	3% Δ	-3% Δ	3% Δ	-3% Δ	3% Δ	-3% Δ	3% Δ	-3% Δ	3% Δ	-3% Δ	3% Δ	-3% Δ	3% Δ
Type-B flow	7	4	2	4	8	4	14	7	2	2	0	2	3	2	0	2	4	3
Type-C flow	10	3	1	2	7	3	13	8	3	3	0	6	4	9	1	3	2	2
Control test	*17*	*2*	*7*	*1*	*14*	*1*	*15*	*5*	*5*	*2*	*0*	*8*	*6*	*5*	*4*	*3*	*4*	*6*

Fig. 5. Boxplots of the OAR doses in the mid-treatment calculated plans compared to the original treatment plans. The figure is complemented by the number of cases in both planning workflows and the Control test, having a ± 3 % dose difference per constraint.

In the OAR constraints, lower maximum doses are noticeable in the Spinal Canal for both planning workflows. Regarding the average dose on the heart, similar trends are observed between the two planning workflows, with almost half of the cases having a 3 % dose decrease, and a third of the cases showing a 3 % dose increase. The mid-treatment Type-C calculations reveal higher doses on critical organs such as the mediastinum and esophagus. The control test demonstrates that Type-B is less sensitive to alterations in these organs, as higher doses are revealed when calculating the plan mid-treatment with Type-C.

Discussion

Our study evaluated the impact of dose calculation algorithm on the decision to adapt based on dosimetric information utilizing mid-treatment sCTs.

During our mid-treatment dosimetric-based plan-adaptation assessment, we observed that transitioning from Type-B to Type-C resulted in opposite decisions in nearly one-third of the cases. Type-C demonstrated greater sensitivity to changes in anatomy compared to Type-B, as evidenced by higher mid-treatment maximum doses in heterogeneous organs such as the esophagus and mediastinal envelope. In general, Type-C more accurately identifies cases for plan-adaptation. Type-B tend to underestimates the dose, as already described in the literature [19,24,35]. An adaptive assessment of Type-B plans with Type-C reveals an increase from 13 to 21 plans that require adaptation. The choice of the dose calculation algorithm influences the outcomes in an adaptive assessment workflow, underscoring the necessity for both baseline planning and adaptive planning to employ the same algorithm. Utilizing the Type-C algorithm in the iterative pre-treatment planning is sufficient in half of the cases to make the plan robust to intra-thoracic variations during treatment. Consequently, on a workload level, only two additional cases required adaptation compared to Type-B. This insight is crucial for medical physicists and dosimetrists. A conservative approach in plan optimization can mitigate high doses at air-tissue boundaries, thereby enhancing robustness to anatomical changes during treatment.

The decision to adapt the plan was based on our own decision-guide model, which relies on literature and our planning wishlist model. A limitation of the model is that it only detects situations where constraints are exceeded. In future, it is necessary to integrate threshold values indicating a dose difference in our decision-model. Our data reveals that in certain cases, various critical organs such as the heart or the spinal canal demonstrate a clinically relevant dose increase of 3 %, which, according to the model's definition, does not always qualify for adaptation as they can still fall below the specified constraint.

In our study, the delineation method and the applied margin recipe could have had an impact on the results of this study. Herein we've created new CTVs and PTVs based on deformed GTVs. When tumor regression is present, new CTV and PTV volumes have a high probability of being covered by the original CTV and PTV volumes. Nevertheless, important OAR will come closer which can be picked up by the decision model. Since we have a good CTV coverage mid-treatment in the Type-C planning workflow, we can suggest a follow-up study investigating whether we could reduce the PTV margin for our LA-NSCLC patients.

Our research solely utilized a single method for generating synthetic-CTs. DIR-MIM employs a free-form cubic spline interpolation algorithm which have been reported to deform in a larger extend or even lead to

unreasonable deformations if the contrast resolution is low [36–39]. This poor soft-tissue differentiation occurs in the mediastinal region. It would be worthwhile to investigate the impact of employing a more conservative deformable image registration algorithm, such as a regularized B-spline algorithm [36,37], on the present findings. The research did not delve into the possibility of utilizing convolutional neural networks for generating sCTs [31], which could have potentially yielded other dosimetric outcomes. The need for a continuous implementation of improved CBCT-imaging, could lead to fewer uncertainties regarding the interpretation of volume changes within DIR and is one of our future objectives.

In addition, we could debate the calculation grid size used in this study. A smaller calculation grid size of 1 mm has demonstrated larger dosimetric differences in an algorithm comparison study within lung SBRT on planningCT. Similar to our study, Huang et al (2015) found that the Type-C algorithm calculated lower PTV doses compared to Type-B. These relative dose differences increased to a larger extent when a smaller calculation grid size was used [23].

Conclusion

In our study, nearly one-third of the cases would have a different decision for mid-treatment plan-adaption when utilizing Type-C instead of Type-B. There was no substantial increase in the total number of plan-adaptations for LA-NSCLC. However, Type-C is more sensitive to altered anatomy during treatment compared to Type-B. Recalculating Type-B plans with the Type-C algorithm revealed an increase from 13 to 21 cases triggering ART.

Declaration of competing interest

The authors declare no conflicts of interest.

Appendix A. Supplementary material

Supplementary data to this article can be found online at https://doi.org/10.1016/j.tipsro.2024.100236.

References

[1] Van Esch A, Tillikainen L, Pyykkonen J, Tenhunen M, Helminen H, Siljamäki S, et al. Testing of the analytical anisotropic algorithm for photon dose calculation. Med Phys 2006;33(11):4130–48. https://doi.org/10.1118/1.2358333.

[2] Hoffmann L, Jørgensen M-B, Muren LP, Petersen JBB. Clinical validation of the Acuros XB photon dose calculation algorithm, a grid-based Boltzmann equation solver. Acta Oncol 2012;51(3):376–85. https://doi.org/10.3109/0284186X.2011.629209.

[3] Hu Y, Byrne M, Archibald-Heeren B, Collett N, Liu G, Aland T. Validation of the preconfigured Varian Ethos Acuros XB Beam Model for treatment planning dose calculations: A dosimetric study. J Appl Clin Med Phys 2020 Oct 17;21(12):27–42.

[4] Møller DS, Khalil AA, Knap MM, Hoffmann L. Adaptive radiotherapy of lung cancer patients with pleural effusion or atelectasis. Radiotherapy Oncol 2014 Mar;110(3):517–22.

[5] Hattu D, Mannens J, Öllers M, van Loon J, De Ruysscher D, van Elmpt W. A traffic light protocol workflow for image-guided adaptive radiotherapy in lung cancer patients. Radiotherapy Oncol 2022 Oct;175:152–8.

[6] Ma C, Tian Z, Wang R, Feng Z, Jiang F, Hu Q, et al. A prediction model for dosimetric-based lung adaptive radiotherapy. Med Phys 2022;49(10):6319–33. https://doi.org/10.1002/mp.15714.

[7] Hoffmann L, Alber M, Jensen MF, Holt MI, Møller DS. Adaptation is mandatory for intensity modulated proton therapy of advanced lung cancer to ensure target coverage. Radiother Oncol 2017;122(3):400–5.

[8] Appel S, Bar J, Alezra D, Ben-Ayun Maoz, Rabin-Alezra T, Honig N, et al. Image-guidance triggered adaptive replanning of radiation therapy for locally advanced lung cancer: an evaluation of cases requiring plan adaptation. Br J Radiol 2020 Jan 1;93(1105).

[9] Bertholet J, Anastasi G, Noble D, Bel A, van Leeuwen R, Roggen T, et al. Patterns of practice for adaptive and real-time radiation therapy (POP-ART RT) part II: Offline and online plan adaption for interfractional changes. Radiother Oncol 2020;153:88–96.

[10] Møller DS, Lutz CM, Khalil AA, Alber M, Holt MI, Kandi M, et al. Survival benefits for non-small cell lung cancer patients treated with adaptive radiotherapy. Radiother Oncol [Internet] 2022;168:234–40.

[11] Hoppen L, Sarria GR, Kwok CS, Boda-Heggemann J, Buergy D, Ehmann M, et al. Dosimetric benefits of adaptive radiation therapy for patients with stage III non-small cell lung cancer. Radiation Oncology 2023 Feb 22;18(1):34.

[12] Sonke JJ, Belderbos J. Adaptive Radiotherapy for Lung Cancer. Semin Radiat Oncol 2010 Apr;20(2):94–106.

[13] Kavanaugh J, Hugo G, Robinson CG, Roach MC. Anatomical adaptation—Early clinical evidence of benefit and future needs in lung cancer. Semin Radiat Oncol 2019 Jul 1;29(3):274–83.

[14] Kwint M, Conijn S, Schaake E, Knegjens J, Rossi M, Remeijer P, et al. Intra thoracic anatomical changes in lung cancer patients during the course of radiotherapy. Radiother Oncol 2014;113(3):392–7.

[15] Varian Medical Systems. Eclipse Algorithms Reference Guide. 2008.

[16] Knöös T, Wieslander E, Cozzi L, Brink C, Fogliata A, Albers D, et al. Comparison of dose calculation algorithms for treatment planning in external photon beam therapy for clinical situations. Phys Med Biol 2006;51(22):5785–807.

[17] Kry SF, Alvarez P, Molineu A, Amador C, Galvin JM, Followill DS. Algorithms Used in Heterogeneous Dose Calculations Show Systematic Differences as Measured With the Radiological Physics Center's Anthropomorphic Thorax Phantom Used for RTOG Credentialing. Int J Radiat Oncol Biol Phys 2013 Jan 1;85(1):e95–100.

[18] Han T, Mikell JK, Salehpour M, Mourtada F. Dosimetric comparison of Acuros XB deterministic radiation transport method with Monte Carlo and model-based convolution methods in heterogeneous media. Med Phys 2011;38(5):2651–64.

[19] Fogliata A, Nicolini G, Clivio A, Vanetti E, Cozzi L. Critical appraisal of acuros XB and anisotropic analytic algorithm dose calculation in advanced non-small-cell lung cancer treatments. Int J Radiat Oncol Biol Phys 2012 Aug 1;83(5):1587–95.

[20] Kan MWK, Leung LHT, Yu PKN. Verification and dosimetric impact of Acuros XB algorithm on intensity modulated stereotactic radiotherapy for locally persistent nasopharyngeal carcinoma. Med Phys 2012;39(8):4705–14. https://doi.org/10.1118/1.4736819.

[21] Zhou C, Bennion N, Ma R, Liang X, Wang S, Zvolanek K, et al. A comprehensive dosimetric study on switching from a Type-B to a Type-C dose algorithm for modern lung SBRT. Radiat Oncol 2017 May 5;12(1).

[22] Chen WZ. Impact of dose calculation algorithm on radiation therapy. World J Radiol 2014;6(11):874.

[23] Huang B, Wu L, Lin P, Chen C. Dose calculation of Acuros XB and anisotropic analytical algorithm in lung stereotactic body radiotherapy treatment with flattening filter free beams and the potential role of calculation grid size. Radiat Oncol 2015;10(1). https://doi.org/10.1186/s13014-015-0357-0.

[24] Han T, Followill D, Mikell J, Repchak R, Molineu A, Howell R, et al. Dosimetric impact of Acuros XB deterministic radiation transport algorithm for heterogeneous dose calculation in lung cancer. Med Phys [Internet] 2013;40(5):051710. https://doi.org/10.1118/1.4802216.

[25] Kry SF, Lye J, Clark CH, Andratschke N, Dimitriadis A, Followill D, et al. Report dose-to-medium in clinical trials where available; a consensus from the Global Harmonisation Group to maximize consistency. Radiother Oncol [Internet] 2021;159:106–11.

[26] Hansen CR, Crijns W, Hussein M, Rossi L, Gallego P, Verbakel W, et al. Radiotherapy Treatment plannINg study Guidelines (RATING): A framework for setting up and reporting on scientific treatment planning studies. Radiother Oncol 2020;153:67–78.

[27] Nestle U, De Ruysscher D, Ricardi U, Geets X, Belderbos J, Pöttgen C, et al. ESTRO ACROP guidelines for target volume definition in the treatment of locally advanced non-small cell lung cancer. Radiother Oncol 2018;127(1):1–5.

[28] Peeters ST, Dooms C, Van Baardwijk A, Dingemans AMC, Martinussen H, Vansteenkiste J, et al. Functional imaging in lung Selective mediastinal node irradiation in non-small cell lung cancer in the IMRT/VMAT era: How to use E(B)US-NA information in addition to PET-CT for delineation? Radiotherapy Oncol 2016;120:273–8.

[29] Dempsey JF, Romeijn HE, Li JG, Low DA, Palta JR. A Fourier analysis of the dose grid resolution required for accurate IMRT fluence map optimization. Med Phys 2005;32(2):380–8.

[30] Berkovic P, Paelinck L, Lievens Y, Gulyban A, Goddeeris B, Derie C, et al. Adaptive radiotherapy for locally advanced non-small cell lung cancer, can we predict when and for whom? Acta Oncol 2015;54(9):1438–44.

[31] Thummerer A, Oria Carmen Seller, Zaffino P, Meijers Artürs, Marmitt Gabriel Guterres, Wijsman R, et al. Clinical suitability of deep learning based synthetic CTs for adaptive proton therapy of lung cancer. Med Phys 2021 Nov 16;48(12):7673–84.

[32] Ruangchan S, Knäusl B, Fuchs H, Georg D, Clausen M. Experimental benchmarking of RayStation proton dose calculation algorithms inside and outside the target region in heterogeneous phantom geometries. Physica Medica 2020 Aug;76:182–93.

[33] Narayanasamy G, Stathakis S, Bosse C, Saenz D, Myers P, Kirby N, et al. Dose calculation comparisons between three modern treatment planning systems. J Med Phys 2020;45(3):143.

[34] Papanikolaou N, Battista JJ, Boyer AL, Kappas C, Klein E, Mackie TR, et al. TISSUE INHOMOGENEITY CORRECTIONS FOR MEGAVOLTAGE PHOTON BEAMS. International Standard Serial Number. 2004;271–7344.

[35] Padmanaban S, Warren S, Walsh A, Partridge M, Hawkins MA. Comparison of Acuros (AXB) and Anisotropic Analytical Algorithm (AAA) for dose calculation in treatment of oesophageal cancer: effects on modelling tumour control probability. Radiat Oncol 2014;9(1):1–6. https://doi.org/10.1186/s13014-014-0286-3.

[36] Fukumitsu N, Nitta K, Terunuma T, Okumura T, Numajiri H, Oshiro Y, et al. Registration error of the liver CT using deformable image registration of MIM Maestro and Velocity AI. BMC Med Imaging 2017;17(1):1–9. https://doi.org/10.1186/s12880-017-0202-z.

[37] Kadoya N, Nakajima Y, Saito M, Miyabe Y, Kurooka M, Kito S, et al. Multi-institutional validation study of commercially available deformable image registration software for thoracic images. Int J Radiat Oncol Biol Phys 2016;96(2):422–31.

[38] Kirby N, Chuang C, Ueda U, Pouliot J. The need for application-based adaptation of deformable image registration. Med Phys 2012 Dec 12;40(1):011702.

[39] Calusi S, Labanca G, Zani M, Casati M, Marrazzo L, Noferini L, et al. A multiparametric method to assess the MIM deformable image registration algorithm. J Appl Clin Med Phys 2019 Mar 28;20(4):75–82.